The work reported in this document was made possible through support extended to the Massachusetts Institute of Technology, Laboratory for Insulation Research, by the Air Force Cambridge Research Laboratories under Contract AF 19(604)-6155 and Air Force Systems Command under Contract AF 33(616)-8353. Reproduction of this report in whole or in part is permitted for any purpose of the United States Government.

Ferroelectricity and the Chemical Bond in Perovskite-Type Oxides

by

Carl W. Nelson

Laboratory for Insulation Research
Massachusetts Institute of Technology
Cambridge, Massachusetts

Contracts: AF 19(604)-6155
AF 33(616)-8353

May, 1963

FERROELECTRICITY AND THE CHEMICAL BOND IN PEROVSKITE-TYPE OXIDES

by

Carl W. Nelson

Laboratory for Insulation Research
Massachusetts Institute of Technology
Cambridge, Massachusetts

Abstract: The occurrence of ferroelectricity and antiferroelectricity in perovskite-type oxides is inadequately explained by the postulate of an ionic model. Such a model with its radius-ratio rules emphasizes the concept of a critical ionic radius at which rattling of cations within their octahedral oxide surroundings begins. A molecular-orbital approach provides additional insight into the nature of these distortions. The formation of π bonds, in addition to the σ bonds in $BaTiO_3$ structures and isomorphous compounds, leads to a strong mutual interaction along a chain. The absence or presence of π bonding perpendicular to the axis of the strong interaction leads to chain alignments that are ferroelectric or antiferroelectric, respectively. The role played by the cuboctahedral-coordinated cation is described. Comparison of the environment of a cation in acid solution and in perovskite-type oxides reveals great similarity of bonding.

By application of group-theoretical methods, a symmetry classification of orbitals is derived for each molecular point group occurring in $BaTiO_3$. Molecular-orbital energy-level diagrams are constructed. The number and classification of the electronic transitions are predicted by means of the selection rules. It is shown that only ions with empty d shells are capable of forming ferro- and antiferroelectric perovskite-type oxides. A discussion of conductivity in these materials is given.

The Stereochemical Problem

In 1958 Orgel[1] correlated the occurrence of ferroelectricity in perovskite-type oxides with stereochemical trends that characterize the higher oxides of the A-subgroup elements. He concluded from a number of these oxides that there is no sharp transition from octahedral to tetrahedral coordination but an instability developing slowly as the metal ion becomes smaller. This instability leads successively to a loosening of the metal ion at the center of the octahedron, to off-center shifts (e. g. , in ferroelectrics and many other oxides), to extensive displacement of oxide ions producing almost trigonal-bypyramidal coordination, and

1) L. E. Orgel, Discussions Faraday Soc. 26, 138 (1958).

finally to tetrahedral coordination. For the transition metal ions with empty d shells of groups IVA, VA, VIA, and VIIA, the contact radius decreases in the approximate order Hf^{4+}, Zr^{4+}, Ta^{5+}, Nb^{5+}, Ti^{4+}, W^{6+}, Mo^{6+}, V^{5+}, Cr^{6+}, Mn^{7+}. Ferroelectrics are largely restricted to crystals containing ions of intermediate size (Ta^{5+}, Nb^{5+}, Ti^{4+}, W^{6+}) in structures that allow the accretion of the distortions of neighboring octahedra to result in a dipole. Larger ions are too stable in regular octahedral environments; small ones form structures so strongly distorted that no phase transition can occur and that the field required for polarization reversal cannot be attained.

The ions Hf^{4+} and Zr^{4+} also exist in coordinations higher than six:[2] ZrO_2 (above 1600°C) and HfO_2 have the eight-coordinated fluorite structure; for ZrO_2 below 1600°C the coordination is about seven; in $ZrSiO_4$, the Zr^{4+} ions are in the eight-coordinated $[Mo(CN)_8]^{4-}$-type arrangement.

Orgel suggested that additional ferroelectrics and antiferroelectrics should be found among cations of a size appropriate for off-center displacement within their oxide octahedra: e.g., the perovskite-type oxides of V^{4+} and Mo^{5+} contain one d electron in the valence shell; Al^{3+} was added because it occurs in octahedral as well as tetrahedral sites.

To the author's knowledge no ferro- and antiferroelectrics of the perovskite type (except their solid solutions with nonferroelectrics) have cations that contain electrons in the d shell (e.g., V^{4+}, Mo^{5+}, Cr^{3+}) or that have a completed d shell (e.g., Sn^{4+}). The simple ionic model with its radius-ratio rules appears inadequate to explain ferroelectric and antiferroelectric distortions fully. Since the bonds in oxide ferroelectrics and antiferroelectrics must have appreciable covalent character,[1, 3] group-theoretical methods, Mulliken's molecular-orbital theory, Pauling's concept of hybridization of atomic orbitals, Pauling's principle of electroneutrality, and other concepts of structural chemistry will be taken into account. Jørgensen's[4-6] principle of local microsymmetry, which utilizes the symmetry

---

2) J. D. Dunitz and L. E. Orgel, "Stereochemistry of Ionic Solids," in "Advances in Inorganic Chemistry and Radiochemistry," H. J. Emeléus and A. G. Sharpe, Eds., Vol. 2, Academic Press, New York, 1960, p. 47.

3) B. Matthias and A. von Hippel, Phys. Rev. 73, 1378 (1948); A. von Hippel, Revs. Modern Phys. 22, 221 (1950); A. R. von Hippel, "Dielectrics and Waves," John Wiley and Sons, New York, 1954, p. 209; H. D. Megaw, "Ferroelectricity in Crystals," Methuen and Co., London, 1957, pp. 126 and 199.

4) C. K. Jørgensen, "Absorption Spectra and Chemical Bonding in Complexes," Pergamon Press, Oxford, 1962, pp. 63 and 170.

5) C. K. Jørgensen, "Chemical Bonding Inferred from Visible and Ultraviolet Absorption Spectra," in "Solid State Physics," F. Seitz and D. Turnbull, Eds., Vol. 13, Academic Press, New York, 1962, pp. 448, 460.

6) C. K. Jørgensen, "Orbitals in Atoms and Molecules," Academic Press, London, 1962, p. 117.

found in the immediate environment of a central atom and which considers the behavior of the orbitals in the bond region between the central atom and its neighboring ligands, supports this approach. For example, the ligand-field absorption spectrum of nickel(II) oxide[4, 6] closely resembles that of the monomeric entity $Ni(H_2O)_6^{2+}$ in solution, and of diluted Ni(II) in MgO. Also, the position of the first electron-transfer band is the same for the monomeric entity $[VO(H_2O)_5]^{2+}$ in solution, for powdered VO_2, and for crystalline $[VO(H_2O)_4(SO_4)] \cdot H_2O$.[7] The distribution of energy levels in such molecular groups is only slightly perturbed by the environment beyond the first coordination sphere. Except in the case of metallic bonding, where molecular orbitals are completely delocalized, the use of partly localized molecular orbitals seems to lead to reasonable results.

Above 130°C, barium titanate(IV) has the cubic perovskite-type structure, each Ti^{4+} ion at the center of six O^{2-} ions that form a regular octahedron and each octahedron linked to six others by sharing corners. This infinite framework encloses large holes occupied by Ba^{2+} ions, each surrounded by twelve equidistant O^{2-} ions located at the corners of a cuboctahedron. The large ions (ratio Ba^{2+}/O^{2-} = 1/3) form a cubic close-packed arrangement, with the small Ti^{4+} ions in octahedral interstices (Fig. 1). At the ferroelectric Curie point ($T_c \approx 126°C$) the structure becomes tetragonal, at ca. 5°C, orthorhombic, and finally near -80°C, rhombohedral. These three types of distortion from regular octahedral coordination involve motion of the Ti^{4+} ion toward a corner, an edge, and a face, respectively of the octahedron (with the neglect of movement of the Ba^{2+} and O^{2-} ions).

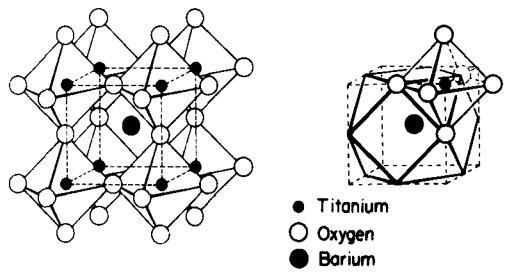

Fig. 1.

Perovskite structure of $BaTiO_3$.

Molecular Orbitals in Cubic $BaTiO_3$

The orbitals primarily involved in σ bonding of the octahedral TiO_6 clusters, which possess O_h symmetry in cubic $BaTiO_3$, are given in Table 1. Figure 2 shows the reference axes for the complex.

Assuming that only σ bonding is operative, the energy-level diagram of Fig. 3

---

7) C. J. Ballhausen and H. B. Gray, Inorg. Chem. 1, 111 (1962).

Table 1. Symmetry classification of orbitals for octahedral coordination (O_h).

Representation	Metal orbitals	Ligand σ orbitals
A_{1g}	4s	$\frac{1}{\sqrt{6}}(\sigma_1+\sigma_2+\sigma_3+\sigma_4+\sigma_5+\sigma_6)$
E_g	$3d_{z^2}$	$\frac{1}{2\sqrt{3}}(2\sigma_5+2\sigma_6-\sigma_1-\sigma_2-\sigma_3-\sigma_4)$
	$3d_{x^2-y^2}$	$\frac{1}{2}(\sigma_1+\sigma_2-\sigma_3-\sigma_4)$
T_{1u}	$4p_x$	$\frac{1}{\sqrt{2}}(\sigma_1-\sigma_2)$
	$4p_y$	$\frac{1}{\sqrt{2}}(\sigma_3-\sigma_4)$
	$4p_z$	$\frac{1}{\sqrt{2}}(\sigma_5-\sigma_6)$
T_{2g}	$3d_{xy}$	
	$3d_{xz}$	
	$3d_{yz}$	

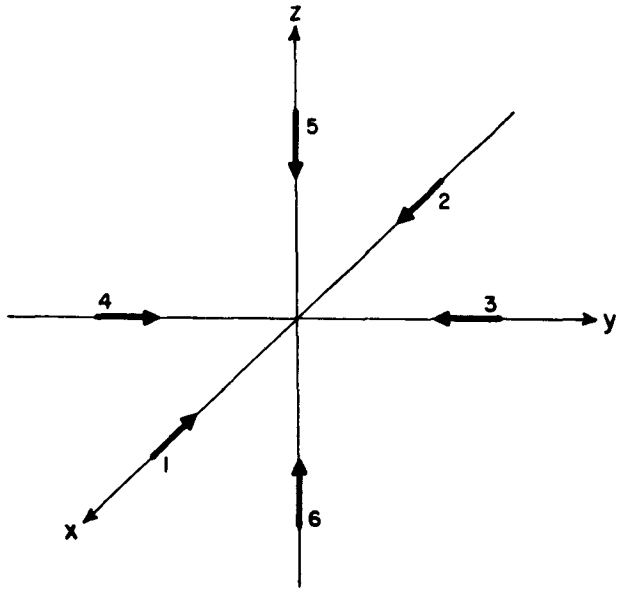

Fig. 2.

Reference axes for σ orbitals of an octahedral cluster (O_h symmetry.

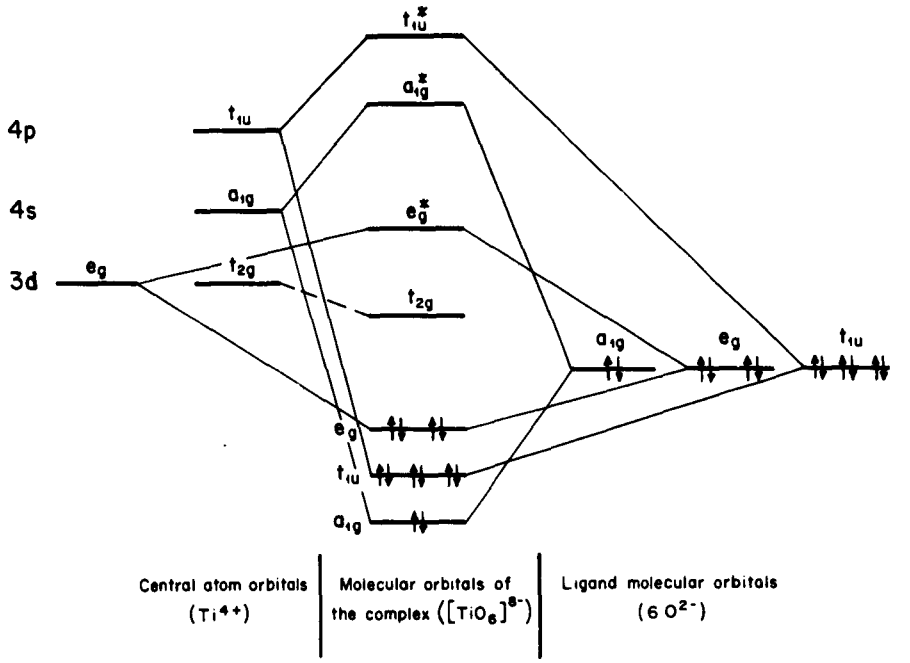

Fig. 3. The molecular-orbital energy-level diagram, assuming only σ bonding, for an octahedral complex (O_h symmetry); (energy not to scale).

may be constructed with the energy levels of the metal ion Ti^{4+} on the left, the molecular orbitals of the ligands (O^{2-} ions) on the right, and the levels for the combined molecular orbitals of the complex $[TiO_6]^{8-}$ in the middle. As long as the ligand orbitals are more stable than the metal ones, a bonding molecular orbital is mainly a ligand orbital while an antibonding molecular orbital is mainly a metal orbital, since a molecular orbital formed from two component orbitals includes a larger contribution from that component which is closer in energy. Since the ligand orbitals are more electronegative than the metal ones, the right-hand energy levels lie below those of the left.

The 2s orbital and one 2p orbital of each O^{2-} ion are hybridized to provide two equivalent sp-directed orbitals in diametrically opposed directions; these form the ligand-σ molecular orbitals involved in bonding to the Ti^{4+} ions. The two remaining 2p orbitals (normal to each other and to the sp-hybrid ones) of each O^{2-} ion are unchanged by the hybridization. If not involved in π bonding with the t_{2g} and t_{1u} orbitals of the Ti^{4+} ions as tacitly assumed in Fig. 3, they must be involved in σ bonding to the Ba^{2+} ions. Six σ bonds involve the Ba^{2+} ion with twelve cuboctahedral-coordinated O^{2-} ions. Since each of the O^{2-} orbitals contains two electrons and the central ion Ti^{4+} is of the noble-gas type, twelve electrons occupy all bonding molecular orbitals in the ground state, and none the non-

Table 2. Symmetry classification of orbitals for octahedral coordination (O_h).

Representation	Metal orbitals	Ligand σ orbitals	Ligand π orbitals
A_{1g}	4s	$\frac{1}{\sqrt{6}}(\sigma_1+\sigma_2+\sigma_3+\sigma_4+\sigma_5+\sigma_6)$	
E_g	$3d_{z^2}$	$\frac{1}{2\sqrt{3}}(2\sigma_5+2\sigma_6-\sigma_1-\sigma_2-\sigma_3-\sigma_4)$	
	$3d_{x^2-y^2}$	$\frac{1}{2}(\sigma_1+\sigma_2-\sigma_3-\sigma_4)$	
T_{1u}	$4p_x$	$\frac{1}{\sqrt{2}}(\sigma_1-\sigma_2)$	$\frac{1}{2}(\pi_{3x}+\pi_{4x}+\pi_{5x}+\pi_{6x})$
	$4p_y$	$\frac{1}{\sqrt{2}}(\sigma_3-\sigma_4)$	$\frac{1}{2}(\pi_{1y}+\pi_{2y}+\pi_{5y}+\pi_{6y})$
	$4p_z$	$\frac{1}{\sqrt{2}}(\sigma_5-\sigma_6)$	$\frac{1}{2}(\pi_{1z}+\pi_{2z}+\pi_{3z}+\pi_{4z})$
T_{2g}	$3d_{xy}$		$\frac{1}{2}(\pi_{1y}-\pi_{2y}+\pi_{3x}-\pi_{4x})$
	$3d_{xz}$		$\frac{1}{2}(\pi_{1z}-\pi_{2z}+\pi_{5x}-\pi_{6x})$
	$3d_{yz}$		$\frac{1}{2}(\pi_{3z}-\pi_{4z}+\pi_{5y}-\pi_{6y})$
T_{2u}			$\frac{1}{2}(\pi_{3x}+\pi_{4x}-\pi_{5x}-\pi_{6x})$
			$\frac{1}{2}(\pi_{1y}+\pi_{2y}-\pi_{5y}-\pi_{6y})$
			$\frac{1}{2}(\pi_{1z}+\pi_{2z}-\pi_{3z}-\pi_{4z})$
T_{1g}			$\frac{1}{2}(\pi_{1y}-\pi_{2y}-\pi_{3x}+\pi_{4x})$
			$\frac{1}{2}(\pi_{1z}-\pi_{2z}-\pi_{5x}+\pi_{6x})$
			$\frac{1}{2}(\pi_{3z}-\pi_{4z}-\pi_{5y}+\pi_{6y})$

bonding t_{2g} orbitals nor the antibonding molecular orbitals.

An alternate description of bonding in cubic $BaTiO_3$ involves rotating each

ligand-π pair of 2p orbitals by 45°, enabling π bonding with the Ti^{4+} t_{2g} and t_{1u} orbitals and making Ba^{2+} completely nonbonded (Table 2, Figs. 4 and 5). There may be resonance between the two structures. Since f orbitals from the central metal atom are not available, the ligand-π t_{2u} molecular orbitals are nonbonding, as are the ligand-π t_{1g} ones, which require g orbitals from the central atom. Because of the infinite three-dimensional framework, the ligand-π orbitals belong not only to one central metal atom but also to the six surrounding ones.

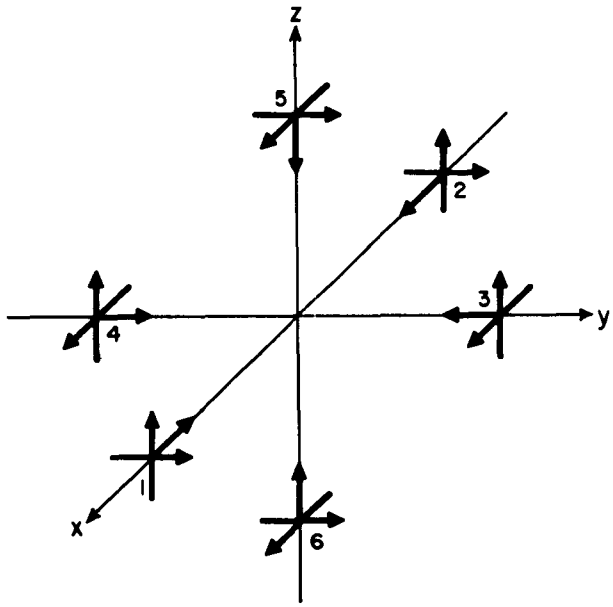

Fig. 4.

Reference axes for σ and π orbitals of an octahedral cluster (O_h symmetry).

Electronic Transitions in Cubic $BaTiO_3$

In the first bonding scheme, electron-transfer (charge-transfer) spectra are caused by transitions from the filled bonding t_{1u} molecular (essentially ligand-σ molecular orbitals) to the empty nonbonding t_{2g} metal orbitals and at higher energy to the empty antibonding e_g^* molecular orbitals (mainly metal orbitals) (cf. Fig. 3). The electronic configuration of the molecular ground state $^1A_{1g}$ is $[(a_{1g})^2(t_{1u})^6(e_g)^4]$. The transitions are represented as:

$$(t_{1u})^6 \rightarrow (t_{1u})^5(t_{2g}): \; ^1A_{1g} \rightarrow {}^1A_{2u} + {}^1E_u + {}^1T_{1u} + {}^1T_{2u},$$

$$(t_{1u})^6 \rightarrow (t_{1u})^5(e_g^*): \; ^1A_{1g} \rightarrow {}^1T_{1u} + {}^1T_{2u}.$$

With increasing energy in the second bonding scheme the electron transitions are from the filled nonbonding t_{2u} molecular orbitals (entirely ligand-π), from the filled weak bonding (nearly nonbonding) t_{1u}^* molecular orbitals (mainly ligand-π with some ligand-σ and a little metal 4p), and from the filled bonding t_{1u} molecular

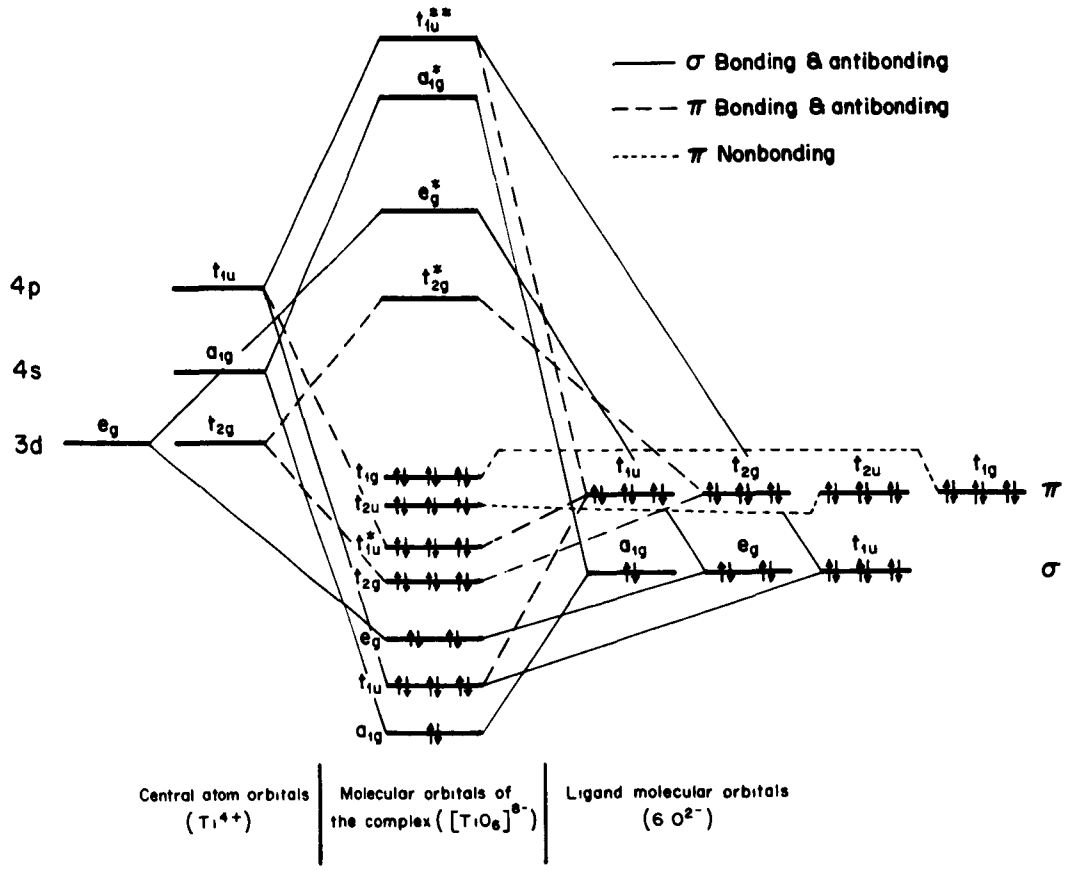

Fig. 5. The molecular-orbital energy-level diagram, for σ and π bonding of an octahedral complex (O_h symmetry); (energy not to scale).

orbitals (mainly ligand-σ with some ligand-π and some metal 4p) to the empty t_{2g}^* and e_g^* antibonding molecular orbitals (mainly metal orbitals) (cf. Fig. 5). These electronic excitations may be represented as follows:

$$(t_{2u})^6 \longrightarrow (t_{2u})^5(t_{2g}^*): \ {}^1A_{1g} \longrightarrow {}^1A_{1u} + {}^1E_u + {}^1T_{1u} + {}^1T_{2u}$$

$$(t_{2u})^6 \longrightarrow (t_{2u})^5(e_g^*): \ {}^1A_{1g} \longrightarrow {}^1T_{1u} + {}^1T_{2u}$$

$$(t_{1u}^*)^6 \longrightarrow (t_{1u}^*)^5(t_{2g}^*): \ {}^1A_{1g} \longrightarrow {}^1A_{2u} + {}^1E_u + {}^1T_{1u} + {}^1T_{2u}$$

$$(t_{1u}^*)^6 \longrightarrow (t_{1u}^*)^5(e_g^*): \ {}^1A_{1g} \longrightarrow {}^1T_{1u} + {}^1T_{2u}$$

$$(t_{1u})^6 \longrightarrow (t_{1u})^5(t_{2g}^*): \ {}^1A_{1g} \longrightarrow {}^1A_{2u} + {}^1E_u + {}^1T_{1u} + {}^1T_{2u}$$

$$(t_{1u})^6 \longrightarrow (t_{1u})^5(e_g^*): \ {}^1A_{1g} \longrightarrow {}^1T_{1u} + {}^1T_{2u}$$

For an allowed transition, the product of the representations of the two interacting states must contain that of the transition-moment operator.[8-12] (Only electric-dipole transitions are considered here. The components of the electric-dipole-moment operator transform like translations x, y, and z.) Since the ground state is $^1A_{1g}$ and the electric-dipole-moment vector of the transitions transforms in O_h as T_{1u}, only the $^1T_{1u}$ excited states are symmetry-allowed. Transitions may also occur, however, between states whose electronic symmetries do not differ in dipole moment provided the interaction between the electronic and vibrational parts of the wave function is considered; if the vibrational x electronic parts obey the symmetry rule, the transition becomes vibronically allowed. The $^1A_{2u}$, ^1E_u, and $^1T_{2u}$ excited states are therefore vibronically allowed, since (from the set of stretching a_{1g}, ϵ_g, τ_{1u} and bending τ_{1u}, τ_{2u}, τ_{2g} vibrational modes in O_h) the ϵ_g and τ_{2g} modes can couple T_{2u} and $A_{2u} + E_u + T_{2u}$, respectively, with T_{1u}. The $^1A_{1u}$ excited state is strictly forbidden. The intensity of the vibronically allowed transitions is between 10^{-4} and 10^{-1} of the symmetry-allowed transitions.

Molecular Orbitals and Electronic Transitions in Tetragonal $BaTiO_3$

The tetragonal distortion from regular octahedral coordination is along the original cubic ⟨100⟩ direction. The resulting molecular geometry belongs to point group C_{4v}. In the molecular-orbital description for the TiO_6 group of C_{4v} symmetry, the 3d, 4s, and 4p orbitals of Ti^{4+} are used for bonding, along with the $\sigma 2s$, $\sigma 2p_z$ ($\sigma 2p_x$ or $\sigma 2p_y$), and $\pi 2p_x$, $\pi 2p_y$ (or $\pi 2p$) orbitals of the O^{2-} ligands. The symmetry classification of the primary-atom and ligand-atom orbitals for point group C_{4v} in the six-coordinate arrangement is adapted from Ballhausen and Gray[7] (Table 3 and Fig. 6) or may be derived from the C_{4v} character table of Wilson et al.[13]

---

8) D. S. McClure, "Electronic Spectra of Molecules and Ions in Crystals," in Solid State Physics," F. Seitz and D. Turnbull, Eds., Vol. 9, Academic Press, New York, 1959, pp. 430 ff.

9) E. B. Wilson, Jr., J. C. Decius, and P. C. Cross, "Molecular Vibrations," McGraw-Hill Book Co., New York, 1962, pp. 156 and 330.

10) C. J. Ballhausen, "Introduction to Ligand Field Theory," McGraw-Hill Book Co., New York, 1962, pp. 170 and 180.

11) A. D. Liehr, J. Chem. Educ. 39, 135 (1962).

12) C. K. Jørgenson, Ref. 4, p. 101.

13) E. B. Wilson, Jr., J. C. Decius, and P. C. Cross, loc. cit. p. 325.

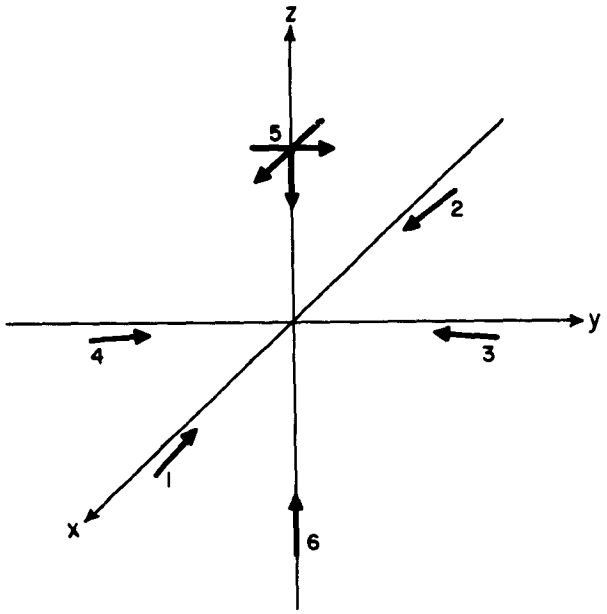

Fig. 6.

Reference axes for σ and π orbitals of a six-coordinate complex belonging to point group C_{4v}.

Table 3. Symmetry classification of orbitals for point group C_{4v} in the six-coordinate arrangement.

Representation	Metal orbitals	Ligand σ orbitals	Ligand π orbitals
A_1	$\frac{1}{\sqrt{2}}(4s + 3d_{z^2})$	σ_5	
	$\frac{1}{\sqrt{2}}(4s - 3d_{z^2})$	$\frac{1}{2}(\sigma_1+\sigma_2+\sigma_3+\sigma_4)$	
	$4p_z$	$-\sigma_6$	
B_1	$3d_{x^2-y^2}$	$\frac{1}{2}(\sigma_1+\sigma_2-\sigma_3-\sigma_4)$	
B_2	$3d_{xy}$		
E	$3d_{xz}$		π_{5x}
	$3d_{yz}$		π_{5y}
	$4p_x$	$\frac{1}{\sqrt{2}}(\sigma_1 - \sigma_2)$	
	$4p_y$	$\frac{1}{\sqrt{2}}(\sigma_3 - \sigma_4)$	

The shortest Ti—O bond (1.869 A) directed along the +z axis is the strongest, and the four Ti—O bonds (1.999 A) to the square-planar arrangement of O^{2-} ligands in the direction of (and slightly below) the $\pm x$ and $\pm y$ axes are equivalent and stronger than the Ti—O bond (2.167 A) directed along the -z axis, which is the weakest of all.[14,15] With a part translation into valence-bond language the bonding can be described as follows: a σ bond of symmetry A_1 between the σ_5 hybrid orbital of O^{2-} and the $[1/\sqrt{2}(4s + 3d_{z^2})]$ hybrid orbital of Ti^{4+}, and two π bonds of symmetry E between the O^{2-} $\pi_5 2p_x$ and $2p_y$ orbitals and the Ti^{4+} $3d_{xz}$ and $3d_{yz}$ orbitals, respectively, making a total of three bonds in TiO^{2+}; four σ bonds involving one σ hybrid orbital from each of the equivalent square-planar O^{2-} ions [i.e., $1/2(\sigma_1 + \sigma_2 + \sigma_3 + \sigma_4)$, $1/\sqrt{2}(\sigma_1 - \sigma_2)$, $1/\sqrt{2}(\sigma_3 - \sigma_4)$, and $1/2(\sigma_1 + \sigma_2 - \sigma_3 - \sigma_4)$] and the $Ti^{4+}[1/\sqrt{2}(4s - 3d_{z^2})]$ hybrid (of symmetry A_1), $4p_x$ and $4p_y$ (of symmetry E), and $3d_{x^2-y^2}$ (of symmetry B_1) orbitals, respectively; a σ bond along the -z axis between the $-\sigma_6$ hybrid orbital of O^{2-} and the Ti^{4+} $4p_z$ orbital of symmetry A_1; and the remaining Ti^{4+} $3d_{xy}$ orbital of symmetry B_2 is nonbonding (cf. Table 3).

Since the Ti—O—Ti angle along the x and y axes is 171°28', the two σ hybrid orbitals of each square-planar O^{2-} ion involve slightly more p character and commensurately less s character (forming $s^{(1-n)/2}p^{(1+n)/2}$ hybrids where $n \simeq 0.02$) than does that of the 180° hybridization. The interorbital angle of the maxima of the pair of π orbitals of each square-planar O^{2-} ion therefore increases from 90° for pure p because of their slight decrease in p character and increase in s character (forming $p^{1-n/2}s^{n/2}$ hybrids). The two pairs of hybrids are in mutually perpendicular planes. In short, the original sp hybridization is on its way to sp^3. The positive lobes of the $s^{(1-n)/2}p^{(1+n)/2}$ pair each have the same +z component, while those of the $p^{1-n/2}s^{n/2}$ pair have the same -z component (of course different in magnitude from that of the +z component). Therefore, the Ba-O distance along the direction of the positive lobe $p^{1-n/2}s^{n/2}$ hybrid orbitals (four of these point toward each Ba^{2+}) ought to be the shortest such distance from Ba^{2+} to the corners of the cuboctahedron; this Ba-O-Ba angle ought to be slightly larger than 90°. This is indeed the case, for the distance along these positive lobe hybrids is 2.800 A, whereas the other distances are 2.824 A to the z-axis O^{2-} ions which have no orbitals available for bonding to Ba^{2+}, and 2.886 A to the square-planar O^{2-} ions along the negative lobe $p^{1-n/2}s^{n/2}$ hybrid orbitals which are largely antibonding. The angle involving the 2.800-A interatomic distance is 90°56'. The

---

14) Interatomic distances and bond angles for tetragonal $BaTiO_3$ are given by H. D. Megaw, "Ferroelectricity in Crystals," Methuen and Co., London, 1957, p. 61, calculated from parameters given by B. C. Frazer, H. R. Danner and R. Pepinsky, Phys. Rev. 100, 745 (1955).

15) For a discussion of the uncertainty in these parameters see H. T. Evans, Jr., Acta Cryst. 14, 1019 (1961), and H. D. Megaw, ibid. 15, 972 (1962).

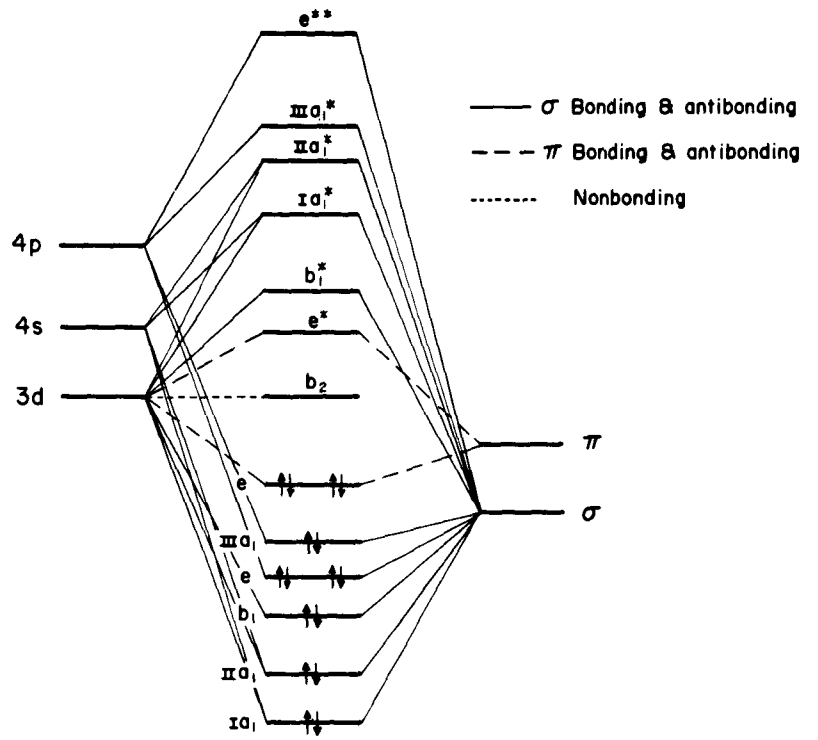

Fig. 7. The molecular-orbital energy-level diagram of a six-coordinate complex of C_{4v} symmetry; (energy not to scale).

order of interatomic distances and the magnitude of the angle are in full agreement with the proposed model. In addition, because the square-planar O^{2-} ligand $p^{1-n/2}s^{n/2}$ hybrid orbitals point toward and are involved in σ bonding with Ba^{2+}, they are not of proper symmetry to overlap with the $3d_{xy}$ orbital of Ti^{4+}, and they do not provide effective overlap with the remaining orbitals of Ti^{4+}. Therefore π bonding involving ligands other than the apical one is of no significance.

An electronic excitation from the filled π-bonding e molecular orbitals (mainly ligand-π) to the empty nonbonding b_2 orbital (metal d_{xy}) (Fig. 7) produces the transition $^1A_1 \rightarrow {}^1E$ which occurs with light polarized perpendicularly to the C_4 axis (the crystallographic c axis) since the electric-dipole-moment vector parallel and perpendicular to the z axis transforms in C_{4v} as A_1 and E, respectively. At higher energy an electronic excitation from the same ground state $^1A_1$ to the empty π-antibonding e* molecular orbitals (largely metal d_{xz} and d_{yz}) gives rise to the excited states $^1A_1 + {}^1A_2 + {}^1B_1 + {}^1B_2$, of which only $^1A_1$ is symmetry-allowed, appearing principally in parallel polarization. The $^1A_2$, $^1B_1$, and $^1B_2$ states are vibronically allowed, since from the set of $4a_1$, $2\beta_1$, β_2, 4ϵ vibrational modes in C_{4v} the β_1 and β_2 modes can couple B_1 and B_2, respectively, with A_1,

while the ϵ modes can couple $A_2 + B_1 + B_2$ with E. The lower intensity $^1A_1 \longrightarrow {}^1B_1$, $^1B_2$ transitions occur both parallel and perpendicular, while the $^1A_1 \longrightarrow {}^1A_2$ transition occurs perpendicular only.

Should this model be correct for tetragonal $BaTiO_3$, these absorption bands in the near ultraviolet will be observed and may be identified. The absorption bands for cuboctahedrally coordinated Ba^{2+} are expected to occur > 50,000 cm^{-1}, as with Ba^{2+} in aqueous solution where Ba^{2+} is coordinated to probably twelve H_2O molecules, unlike the bands in octahedrally coordinated Ba^{2+} in BaO, where they occur at 33,100 and 35,300 cm^{-1}. Jørgensen[16] shows that O^{2-} anions need close packing to be stabilized; they are very reducing for large and very stable for small interanionic distances. Consequently, absorption in BaO involves excitation of only the O^{2-} anions of the type $2s^22p^6 \longrightarrow 2s^22p^53s$. Since the O^{2-} anions are close-packed around the large Ba^{2+} cation in $BaTiO_3$, absorption is not expected to occur until much higher energy is reached. Such absorption therefore will not interfere with the $(e_\pi)^4 \longrightarrow (e_\pi)^3(b_2)$ and $(e_\pi)^4 \longrightarrow (e_\pi)^3(e_\pi^*)$ transitions of Fig. 7.

Molecular Orbitals and Electronic Transitions in Orthorhombic $BaTiO_3$

The orthorhombic distortion from regular octahedral coordination is here along the original cubic ⟨110⟩ direction. The resulting molecular geometry belongs to point group C_{2v}. The allowed combinations of the primary-atom and six ligand-atom orbitals for σ- and π-bond formation are derived from the C_{2v} character table of Wilson et al.[13] The six σ representations are $3A_1 + 2B_1 + B_2$, and the four π representations are $A_1 + A_2 + B_1 + B_2$ (Table 4 and Fig. 8).

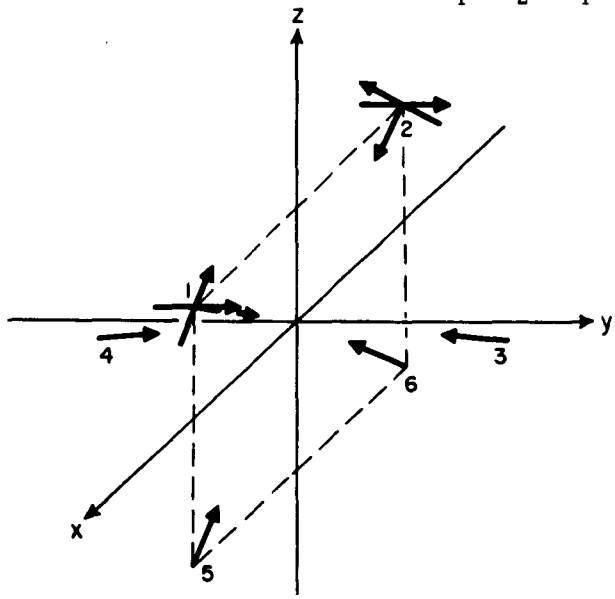

Fig. 8.

Reference axes for σ and π orbitals of a six-coordinate complex belonging to point group C_{2v}.

16) C. K. Jørgensen, cf. Ref. 4, p. 168, and Ref. 5, p. 440.

Table 4. Symmetry classification of orbitals for point group C_{2v} in the six-coordinate arrangement.

Representation	Metal orbitals	Ligand σ orbitals	Ligand π orbitals
A_1	$\frac{1}{\sqrt{5}}(3d_{z^2}) + \frac{2}{\sqrt{5}}(4s)$	$\frac{1}{\sqrt{2}}(\sigma_1 + \sigma_2)$	
	$\frac{2}{\sqrt{5}}(3d_{z^2}) - \frac{1}{\sqrt{5}}(4s)$		$\frac{1}{\sqrt{2}}(\pi_{1xz} + \pi_{2xz})$
	$3d_{x^2-y^2}$	$\frac{1}{\sqrt{2}}(-\sigma_3 - \sigma_4)$	
	$4p_z$	$\frac{1}{\sqrt{2}}(-\sigma_5 - \sigma_6)$	
A_2	$3d_{xy}$		$\frac{1}{\sqrt{2}}(\pi_{1y} - \pi_{2y})$
B_1	$3d_{xz}$	$\frac{1}{\sqrt{2}}(\sigma_1 - \sigma_2)$	
	$4p_x$	$\frac{1}{\sqrt{2}}(\sigma_5 - \sigma_6)$	$\frac{1}{\sqrt{2}}(-\pi_{1xz} + \pi_{2xz})$
B_2	$4p_y$	$\frac{1}{\sqrt{2}}(\sigma_3 - \sigma_4)$	
	$3d_{yz}$		$\frac{1}{\sqrt{2}}(\pi_{1y} + \pi_{2y})$

The equivalent Ti-O bonds of 1.904 A,[17] 47°21' from the z axis to ligands 1 and 2 in the xz plane (cf. Fig. 8), are the strongest ones, those of 1.998 A, 93°15' from the z axis to ligands 3 and 4 in the yz plane, are intermediate, and those of 2.113 A, 42°45' from the -z axis to ligands 5 and 6 in the xz plane, are the weakest.

The pair of 2p orbitals of π symmetry on each yz-plane O^{2-} ion is omitted in Table 4 for the following reason: Since the Ti-O-Ti angle along the y axis is 173°29', the two σ hybrid orbitals of each O^{2-} ion in the yz plane involve slightly more p character and thus less s character (forming $s^{(1-n)/2}p^{(1+n)/2}$ hybrids where $n \simeq 0.02$) than does that of the 180° hybridization. The interorbital angle of the maxima of the pair of π orbitals therefore increases from 90° for pure p

17) Interatomic distances and bond angles for orthorhombic $BaTiO_3$ calculated from parameters given by G. Shirane, H. Danner, and R. Pepinsky, Phys. Rev. 105, 856 (1957).

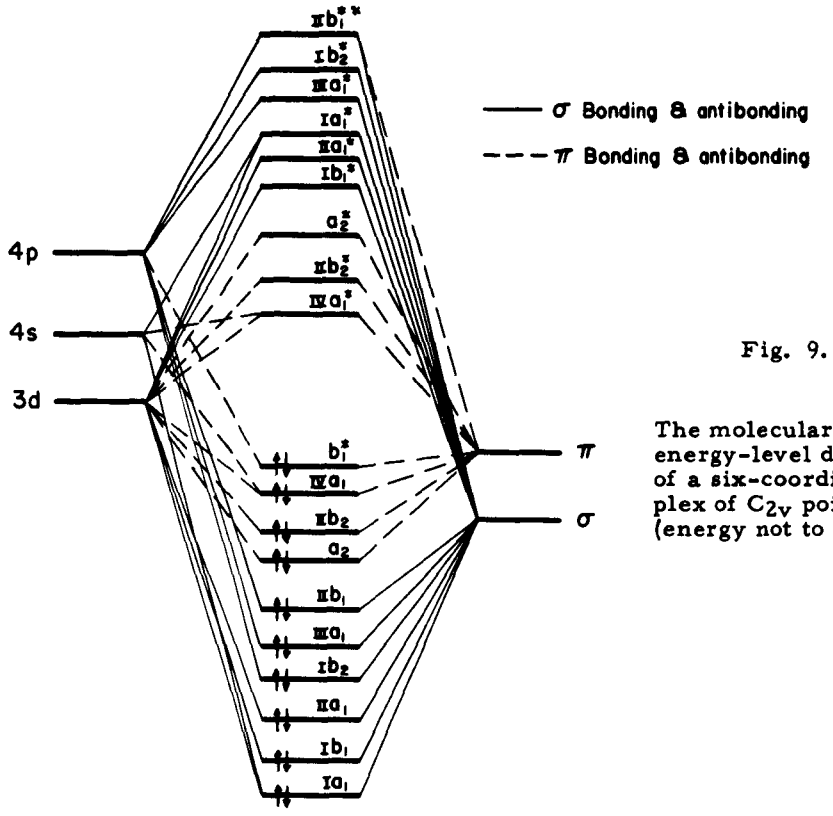

Fig. 9.

The molecular-orbital energy-level diagram of a six-coordinate complex of C_{2v} point group; (energy not to scale).

because of their slight decrease in p and increase in s character (forming $p^{1-n/2}\,s^{n/2}$ hybrids). The two pairs of hybrids are in mutually perpendicular planes. In short, the original sp hybridization is on its way to sp^3. The positive lobes of the $p^{1-n/2}\,s^{n/2}$ hybrid pair are directed slightly more than 45° away from the -z direction. Therefore, these orbitals point between the Ba^{2+} ions and do not provide effective overlap with any of the Ti^{4+} orbitals.

The ordering of molecular orbitals in Fig. 9 is based on qualitative concepts: The σ-bonding molecular orbitals lie deeper than the π-bonding ones because the partners of the former are directed more toward one another than those of the latter; for the same reason the σ-antibonding ones lie higher than the π-antibonding ones. Within these groupings the ordering of levels is predicated, too, on the overlap criterion. For example, among the π-bonding molecular orbitals, the greater overlap (the $O_{(1)}$-Ti-$O_{(2)}$ angle is $> 90^\circ$) of the combination in a_2 (cf. Table 4 and Fig. 9) than in b_2 places the former below the latter. The normalization coefficients of the $3d_{z^2}$-4s hybrid orbital (Table 4) are chosen by requiring its node to be 47° from the z axis and thus pass through the O^{2-} position ($O_{(1)}$ and $O_{(2)}$), so that the positive and negative lobes of the O^{2-} πp orbitals

overlap in the corresponding regions of the hybrid. The overlap of the combination in b_1^* is the least, because while one lobe of each O^{2-} p orbital dips into a lobe of Ti^{4+} $4p_x$, the other points away into a region where $4p_x$ is of low density and opposite sign. Furthermore, since Ti^{4+} $4p_x$ is involved in the σ-bonding b_1 molecular orbital, b_1^* is nearly π-nonbonding and lies higher than the stronger π-bonding ones. In addition, the pair of triple bonds to ligands 1 and 2 in orthorhombic $BaTiO_3$ is expected to be somewhat longer than the single triple bond in tetragonal $BaTiO_3$. Compare the orthorhombic 1.904-A distance with the tetragonal 1.869-A one.

Since the electric-dipole-moment vector parallel to the x, y, and z axes transforms in C_{2v} as B_1, B_2, and A_1, respectively, and the ground state is $^1A_1$, the symmetry-allowed electronic transitions from the filled weak and strong π-bonding molecular orbitals to the empty π-antibonding ones (Cf. Fig. 9) are as follows:

$$(b_1^*)^2 \longrightarrow (b_1^*)(IVa_1^*): \quad {}^1A_1 \longrightarrow {}^1B_1 \quad (\parallel x)$$

$$(b_1^*)^2 \longrightarrow (b_1^*)(a_2^*): \quad {}^1A_1 \longrightarrow {}^1B_2 \quad (\parallel y)$$

$$(IVa_1)^2 \longrightarrow (IVa_1)(IVa_1^*): \quad {}^1A_1 \longrightarrow {}^1A_1 \quad (\parallel z)$$

$$(IVa_1)^2 \longrightarrow (IVa_1)(IIb_2^*): \quad {}^1A_1 \longrightarrow {}^1B_2 \quad (\parallel y)$$

$$(IIb_2)^2 \longrightarrow (IIb_2)(IVa_1^*): \quad {}^1A_1 \longrightarrow {}^1B_2 \quad (\parallel y)$$

$$(IIb_2)^2 \longrightarrow (IIb_2)(IIb_2^*): \quad {}^1A_1 \longrightarrow {}^1A_1 \quad (\parallel z)$$

$$(IIb_2)^2 \longrightarrow (IIb_2)(a_2^*): \quad {}^1A_1 \longrightarrow {}^1B_1 \quad (\parallel x)$$

$$(a_2)^2 \longrightarrow (a_2)(IIb_2^*): \quad {}^1A_1 \longrightarrow {}^1B_1 \quad (\parallel x)$$

$$(a_2)^2 \longrightarrow (a_2)(a_2^*): \quad {}^1A_1 \longrightarrow {}^1A_1 \quad (\parallel z)$$

The x, y, and z axes of point group C_{2v} correspond to the crystallographic orthorhombic axes a, b, and c, respectively, of space group Bmm2.

Molecular Orbitals and Electronic Transitions in Rhombohedral $BaTiO_3$

The rhombohedral distortion from regular octahedral coordination is here along the original cubic ⟨111⟩ direction. The resulting molecular geometry belongs to point group C_{3v}. The allowed combinations of primary-atom and six ligand-atom orbitals for σ- and π-bond formation are derived from the C_{3v} character table of Wilson et al.[13] The six σ representations are $2A_1 + 2E$, and

Table 5. Symmetry classification of orbitals for point group C_{3v} in the six-coordinate arrangement.

Representation	Metal orbitals	Ligand σ orbitals	Ligand π orbitals
A_1	$3d_{z^2}$		$\frac{1}{\sqrt{6}}(\pi_{1'} + \pi_{1''} + \pi_{2'} + \pi_{2''} + \pi_{3'} + \pi_{3''})$
	$4s$	$\frac{1}{\sqrt{3}}(\sigma_1 + \sigma_2 + \sigma_3)$	
	$4p_z$	$\frac{1}{\sqrt{3}}(-\sigma_4 - \sigma_5 - \sigma_6)$	
A_2			$\frac{1}{\sqrt{6}}(\pi_{1'} - \pi_{1''} + \pi_{2'} - \pi_{2''} + \pi_{3'} - \pi_{3''})$
E	$3d_{xz}$	$\frac{1}{\sqrt{6}}(2\sigma_1 - \sigma_2 - \sigma_3)$	
	$3d_{yz}$	$\frac{1}{\sqrt{2}}(\sigma_2 - \sigma_3)$	
	$3d_{x^2-y^2}$		$\frac{1}{2}(-\pi_{2'} + \pi_{2''} + \pi_{3'} - \pi_{3''})$
	$3d_{xy}$		$\frac{1}{2\sqrt{3}}(-2\pi_{1'} + 2\pi_{1''} + \pi_{2'} - \pi_{2''} + \pi_{3'} - \pi_{3''})$
	$4p_x$	$\frac{1}{\sqrt{6}}(-2\sigma_4 + \sigma_5 + \sigma_6)$	$\frac{1}{2\sqrt{3}}(-2\pi_{1'} - 2\pi_{1''} + \pi_{2'} + \pi_{2''} + \pi_{3'} + \pi_{3''})$
	$4p_y$	$\frac{1}{\sqrt{2}}(\sigma_5 - \sigma_6)$	$\frac{1}{2}(-\pi_{2'} - \pi_{2''} + \pi_{3'} + \pi_{3''})$

the six π representations are $A_1 + A_2 + 2E$ (Table 5 and Fig. 10). The equivalent Ti-O bonds directed upward to ligands 1, 2, and 3 are the shorter and stronger ones, while those directed downward to ligands 4, 5, and 6 are the longer and weaker ones. The Ba^{2+} ions are not involved in σ bonding, since all of the πp orbitals of the ligand O^{2-} ions point between them.

To the extent that the angle of the Ti-O bonds involving ligands 1, 2, and 3 is $> 54^{\circ}44'$ with respect to the z axis (C_3 axis), 4s may mix with $3d_{z^2}$ to form a hybrid whose node passes through the ligand positions so that the positive and negative lobes of the ligand πp orbitals overlap in the corresponding regions of the

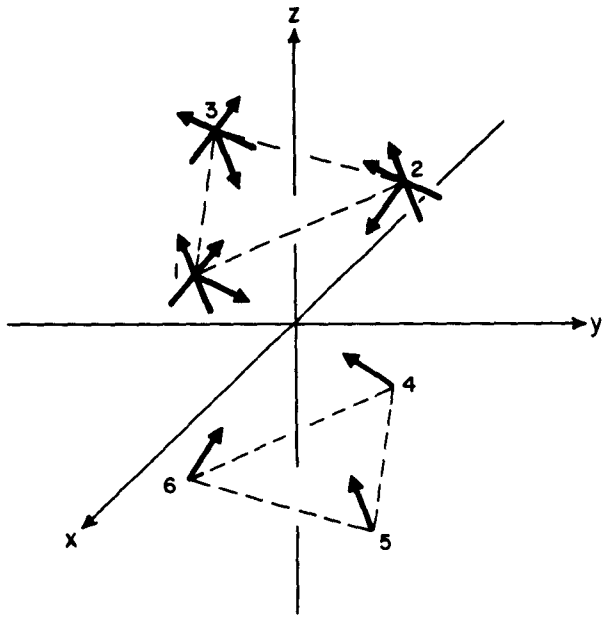

Fig. 10.

Reference axes for σ and π orbitals of a six-coordinate complex belonging to point group C_{3v}.

hybrid. The overlaps of the remaining π combinations are much smaller because the signs of the participating orbitals are not matched everywhere in space. Moreover, since the Ti^{4+} $4p_x$ and $4p_y$ are involved in the σ-bonding IIe molecular orbital, IIe* is nearly π-nonbonding and lies higher than π-bonding IIIe. The a_2 molecular orbital is π-nonbonding and therefore lies between the π-bonding and π-antibonding ones. In addition, the bonds are expected to be somewhat longer than in orthorhombic $BaTiO_3$. A qualitative ordering of levels based on such considerations is given in Fig. 11.

Since the electric-dipole-moment vector parallel and perpendicular to the crystallographic hexagonal c axis (the z axis) transforms in C_{3v} as A_1 and E, respectively, and the ground state is $^1A_1$, the symmetry-allowed transitions from the filled non-, weak, and strong π-bonding molecular orbitals to the empty π-antibonding ones (cf. Fig. 11) are as follows.

$$(a_2)^2 \longrightarrow (a_2)(IIIe^*): \quad {}^1A_1 \longrightarrow {}^1E \qquad (\perp)$$

$$(IIe^*)^2 \longrightarrow (IIe^*)(IIIe^*): \quad {}^1A_1 \longrightarrow {}^1A_1 + {}^1E \qquad (\parallel \text{and} \perp)$$

$$(IIe^*)^2 \longrightarrow (IIe^*)(IIIa_1^*): \quad {}^1A_1 \longrightarrow {}^1E \qquad (\perp)$$

$$(IIIe)^2 \longrightarrow (IIIe)(IIIe^*): \quad {}^1A_1 \longrightarrow {}^1A_1 + {}^1E \qquad (\parallel \text{and} \perp)$$

$$(IIIe)^2 \longrightarrow (IIIe)(IIIa_1^*): \quad {}^1A_1 \longrightarrow {}^1E \qquad (\perp)$$

$$(IIIa_1)^2 \longrightarrow (IIIa_1)(IIIe^*): \quad {}^1A_1 \longrightarrow {}^1E \qquad (\perp)$$

$$(IIIa_1)^2 \longrightarrow (IIIa_1)(IIIa_1^*): \quad {}^1A_1 \longrightarrow {}^1A_1 \qquad (\parallel)$$

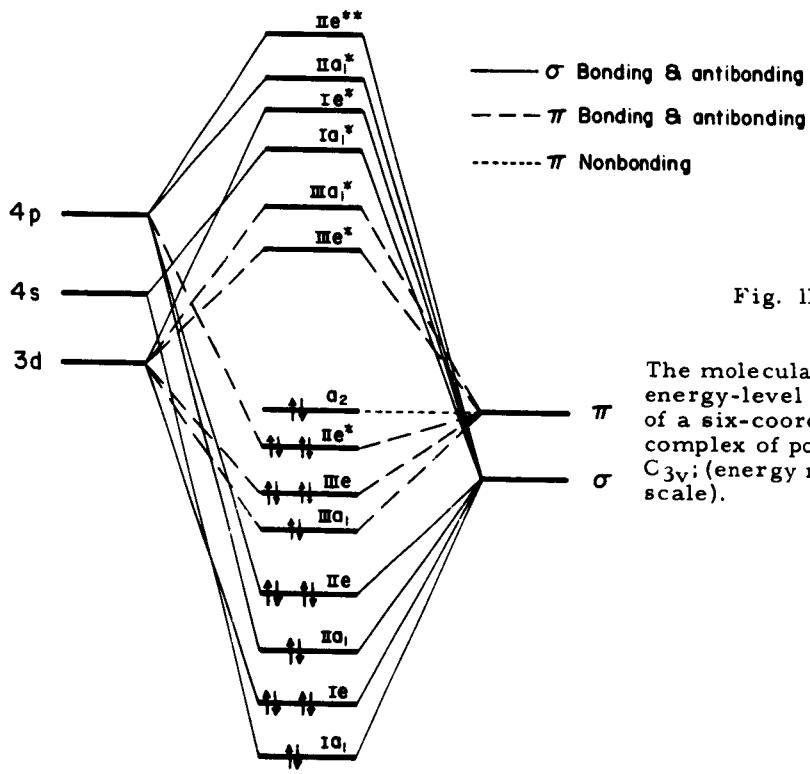

Fig. 11.

The molecular-orbital energy-level diagram of a six-coordinate complex of point group C_{3v}; (energy not to scale).

Comparison with Molecular Species in Solution

In strongly acidic aqueous solution Ti^{4+} occurs as the monomeric molecular ion $[TiO]^{2+}$, since the group is invariably brought into the lattice when a salt crystallizes. In solution five H_2O molecules are presumably bound to the species to complete the six-coordinate arrangement $[TiO(H_2O)_5]^{2+}$ of C_{4v} symmetry. Anions of the ionic medium may replace some of the solvent molecules of the coordination sphere, but the $[TiO]^{2+}$ part always retains its identity. Physiochemical evidence indicates that of all anions perchlorate $(ClO_4)^{1-}$ possesses the least tendency to form complexes with metal ions; nitrate $(NO_3)^{1-}$ is next in this respect. This property and the fact that perchloric and nitric acids are very strong may be explained by the valence theory. For example, the central ion Cl^{7+}, because of

its high oxidation state (+7) and its small ionic radius (0.26 A), polarizes the four ligand O^{2-} ions, thereby transferring charge to the region within the molecule, forming strong covalent σ and π bonds. The σ and π orbitals of the oxygens are involved in bonding with those belonging to the symmetry representations $A_1 + T_2$ and $E + T_2$, respectively, of the central chlorine atom. Since the oxygens of $(ClO_4)^-$ are less negatively charged (i. e., they are in the outward direction more electronegative and therefore poorer electron donors) and have fewer orbitals available for bonding with cations than those of any other anions, the acid strength of perchloric acid and the non-complex-forming property of the perchlorate ion are explained. A similar argument may be given for $(NO_3)^{1-}$ of D_{3h} instead of T_d symmetry.

Summarizing, the actual electron distribution within a molecule or crystal does not correspond to a charge distribution, which equals the oxidation-state number [defined as the charge left on atoms when the ligands (the more electronegative partner in a bond) are assigned the closed-shell inert-gas configuration] of the component ions, but rather to one that approaches electroneutrality. This is Pauling's[18] principle of electroneutrality, which suggests that in stable molecules and crystals the charge associated with each atom stays within -1 to +1. The concept has only an approximate physical meaning because of the ambiguity in partitioning the overlap charge in a bond between the partner atoms.[19] The degree of covalency of bonds increases as the oxidation number increases and as the ionic radius decreases of the primary ion and also with increasing polarizability of the ligands. The study of electron-transfer spectra by Jørgensen[20] suggests that the effective atomic charge of a given element increases little with increasing oxidation number, probably about 0.1 to 0.2 unit per step increase.

Chloride and sulfate $(SO_4)^{1-}$ ions, which are better coordinating agents (this, too, may be understood in terms of the valence theory), may displace some of the water molecules in the coordination sphere of $[TiO(H_2O)_5]^{2+}$; the tendency of an anion to do so also depends on its concentration. Oxalate $(C_2O_4)^{2-}$ and 2,4-pentanedione, which are excellent coordinating agents, displace only the waters of $[TiO(H_2O)_5]^{2+}$. Since the $[TiO]^{2+}$ group remains intact, its electron-transfer bands are not affected by substitution of anions in the coordination sphere. It would indeed be valuable to compare the spectra of tetragonal $BaTiO_3$ with $[TiO(H_2O)_5]^{2+}$ in acid solution and with crystalline $TiO(C_5H_7O_2)_2$, where $C_5H_8O_2$

---

18) L. Pauling, "The Nature of the Chemical Bond," 3rd ed., Cornell University Press, Ithaca, New York, 1960, pp. 172 and 320.

19) C. A. Coulson, Discussions Faraday Soc. 19, 65 (1955); L. E. Orgel, "An Introduction to Transition-Metal Chemistry: Ligand-Field Theory," Methuen and Co., London, 1960, p. 114.

20) C. K. Jørgensen, cf. Ref. 5, pp. 425, 433, and 457; Ref. 6, p. 85.

is 2,4-pentanedione, and also with crystalline $K_2[TiO(C_2O_4)_2]$. The structures of the two latter compounds have not been determined. If Ti^{4+} has a microsymmetry of C_{4v}, their spectra should resemble that of $BaTiO_3$.

The resistance of $[TiO(H_2O)_5]^{2+}$ to protonation may be understood in terms of the polarizing power or electron-withdrawing tendency of Ti^{4+}. (The electron-withdrawing tendency of an ion increases as the electronegativity increases as a function of increasing oxidation number and decreasing ionic radius.) Here Ti^{4+} withdraws charge from one oxygen of a hypothetical $[Ti(H_2O)_6]^{4+}$ ion, making that oxygen positive with respect to the others with the release of two protons and and the reduction of the effective atomic charge of Ti^{4+} (Pauling's electroneutrality principle) and forming covalent bonds where the σ hybrid and πp orbitals of that oxygen become involved in bonding with the appropriate orbitals of Ti^{4+} (Figs. 6, 7 and Table 3). In addition, since s character tends to concentrate in orbitals occupied by unshared electrons (lone pairs), where the low potential energy-space characteristic of an s orbital is used to greater advantage,[21] the digonal hybridization of that oxygen is such that the nonequivalent σ-hybrids $s^{(1/2)-n}p^{(1/2)+n}$ and $s^{(1/2)+n}p^{(1/2)-n}$ (where $0 > n < 1/2$) directed toward and away from Ti^{4+}, respectively, are formed. The increase in s character of the oxygen hybrid-σ-atomic orbital directed away diminishes the electron-donor strength (or the proton-acceptor ability) of the system, leading to an increase in acid strength (or a decrease in base strength), and in ionization potential (or in electronegativity), making that orbital less suitable energetically for bonding.

These concepts for molecular species in solution provide the key for the understanding of ferroelectric and antiferroelectric distortions which lead to one-dimensional cooperative ordering (i.e., the off-center displacement of each cation is in the direction of the chain) in perovskite-type oxides. For example, the principal features of bonding of $[TiO]^{2+}$ in tetragonal $BaTiO_3$ and of $[TiO(H_2O)_5]^{2+}$ in aqueous solution are analogous even to the extent that the square-planar O^{2-} ions of the former and the H_2O molecules of the latter participate in σ bonding but not in π bonding with Ti^{4+}. When a triple bond (a σ and a pair of π bonds) is formed between a Ti^{4+} and an O^{2-} ion, the s character of the O^{2-} ion's σ orbital pointing away must increase, resulting in an increase in length of the remaining bond formed by that O^{2-} ion. Since the longer bond is formed from an orbital less suitable energetically for bonding, it is essentially of ionic character. In $BaTiO_3$ the O^{2-} ion is colinearly attached to two Ti^{4+} ions, forming a triple bond of largely covalent character with one, and a σ bond of largely ionic character with the other. The latter Ti^{4+} ion in the direction opposite to the

---

21) H. A. Bent, J. Chem. Educ. 37, 616 (1960); C. A. Coulson, "Valence," 2nd ed., Oxford University Press, London, 1961, pp. 142 and 218; G. H. Stewart and H. Eyring, J. Chem. Educ. 35, 550 (1958).

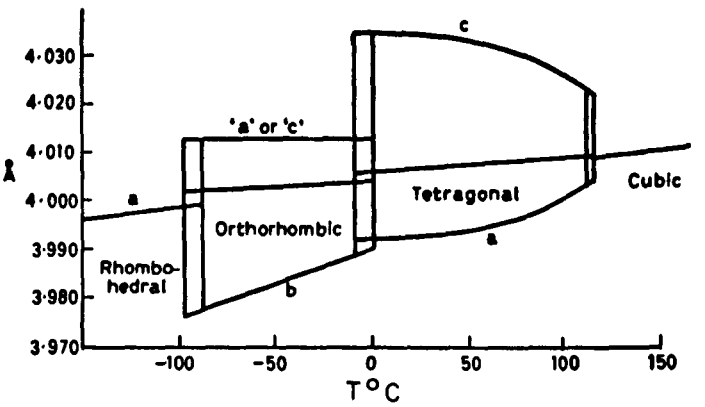

Fig. 12. Variations with temperature of cell edges and cube root of cell volume of $BaTiO_3$. (After Kay and Vousden.[22])

ionic bond has orbitals available for the formation of a triple bond with a second O^{2-} ion. Consequently, the Ti^{4+} displacement caused by the formation of such bonds in one octahedron produces an identical displacement in the same direction for each Ti^{4+} in the chain. The long-range interactions of the Lorentz field are not needed for this structural theory of ferroelectricity. Furthermore, layer-type perovskite oxides that have only two, three, or four octahedra in a chain between the $[Bi_2O_2]^{2+}$ layers are ferroelectric.

Three transitions other than the 1460°C hexagonal-to-cubic one take place in $BaTiO_3$: cubic $\xrightarrow{126°C}$ tetragonal $\xrightarrow{5°C}$ orthorhombic $\xrightarrow{-80°C}$ rhombohedral, where the site symmetry of Ti^{4+} changes from $O_h \longrightarrow C_{4v} \longrightarrow C_{2v} \longrightarrow C_{3v}$, respectively. As the cell volume decreases on cooling (Fig. 12),[22] the overlap of the σ and π orbitals of the O^{2-} ions with those of Ti^{4+} and Ba^{2+} (Table 1 and Fig. 3), respectively, or with those of only Ti^{4+} (Table 2 and Fig. 5) increases in O_h symmetry. To avoid that the effective atomic charge of Ti^{4+} and indeed that of Ba^{2+} are reduced too far (Pauling's electroneutrality principle), as would be the case if O_h symmetry were maintained, the symmetry changes with decreasing temperature. Orbitals of appropriate symmetry of Ti^{4+} overlap with the pair of πp orbitals on one oxygen in C_{4v}, on each of two oxygens sharing an edge in C_{2v}, and on each of three oxygens sharing a face in C_{3v}, resulting in a formation opposite the triple bonds of one, two, and three predominantly ionic σ bonds, respectively. With decreasing temperature and cell volume the overlap and number of oxygen π orbitals, which increase with those of Ti^{4+}, is compensated by an increasing number of ionic bonds, so that the effective atomic charge of Ti^{4+} is not appreciably changed. For Ba^{2+}, six πp oxygen orbitals may participate in σ bonding in O_h, four must

22) H. F. Kay and P. Vousden, Phil. Mag. [7] 40, 1019 (1949).

Table 6. Ionic radii, electronegativity, and molecular ionic species in acid solution.

Ion	Pauling[23] crystal ionic radius (A)		Electronegativity value on Pauling scale[24]	Molecular species in aqueous solution at pH < 1	Symmetry of metal ion
Ti^{4+}	0.68		1.6	$[TiO(H_2O)_5]^{2+}$	C_{4v}
Zr^{4+}	0.80		1.5	$[Zr_4(OH)_8(H_2O)_{16}]^{8+}$	D_{4d}
Hf^{4+}			1.4	$[Hf_4(OH)_8(H_2O)_{16}]^{8+}$	D_{4d}
V^{5+}	0.59		1.9	$[VO_2(H_2O)_3]^{1+}$	D_{3h}
Nb^{5+}	0.70		1.7	$[NbO(H_2O)_5]^{3+}$	C_{4v}
Ta^{5+}			1.7	$[TaO(H_2O)_5]^{3+}$	C_{4v}
Cr^{6+}	0.52		2.3	$[Cr_2O_7]^{2-}$	C_{3v}
Mo^{6+}	0.62		2.1	$[MoO_2(H_2O)_{4 \text{ or } 3}]^{2+}$	$D_{4h \text{ or } 3h}$
W^{6+}			2.0	$[WO_2(H_2O)_4]^{2+}$	D_{4h}
Mn^{7+}	0.46		2.5	$[MnO_4]^{1-}$	T_d
Al^{3+}	0.50		1.5	$[Al(H_2O)_6]^{3+}$	O_h
Sn^{4+}	0.70		1.8	$[Sn(H_2O)_6]^{4+}$	O_h
	CN6	CN12	---		
Na^{+}	0.95	1.07	0.9	$\sim 8H_2O$	
K^{+}	1.33	1.45	0.8	$\sim 12H_2O$	
Rb^{+}	1.48	1.60	0.8	$\sim 12H_2O$	
Cs^{+}	1.69	1.80	0.75	$\sim 14H_2O$	
Ca^{2+}	0.99	1.08	1.0	$\sim 8H_2O$, $[Ca(H_2O)_8]^{2+}$	D_{4d}
Sr^{2+}	1.13	1.22	1.0	$\sim 9H_2O$, $[Sr(H_2O)_{9,8}]^{2+}$	$D_{3h \text{ or } 4d}$
Ba^{2+}	1.35	1.44	0.9	$\sim 12H_2O$	
La^{3+}	1.15	1.23	1.1	$\sim 9H_2O$, $[La(H_2O)_9]^{3+}$	D_{3h}

23) L. Pauling, Ref. 18, pp. 514 and 537 ff.

24) L. Pauling, Ref. 18, pp. 88 ff; W. Gordy and W. J. Orville-Thomas, J. Chem. Phys. 24, 439 (1956).

participate in C_{4v}, none in C_{2v} nor in C_{3v}. The Ti^{4+} displacements along the C_4, C_2, or C_3 axes corresponding to the original cubic ⟨100⟩, ⟨110⟩, or ⟨111⟩ directions, respectively, are mutually dependent and in the same direction, since s character tends to concentrate in each O^{2-} ion's σ orbital opposite those involved in a triple bond. Because of the absence of π bonding perpendicular to the axis of the strong interaction, the alignment of chains in $BaTiO_3$ leads to ferroelectricity. The spontaneous polarization ensuing at the phase transition is a by-product of these effects.

The molecular ionic species that occurs in aqueous solution at pH < 1 for each element in its highest oxidation state of periodic groups IVA, VA, VIA, and VIIA is shown in Table 6. The electron donor (or base) strength of the isoelectronic sequence $H_3O^+ < H_2O < OH^- < O^{2-}$ increases with increasing p character of the orbitals occupied by unshared electron pairs. Hence in acid solution, water molecules are favored in the coordination sphere of a cation. Consider the behavior in acid solution of, for example, the ion series with the Ar structure: K^+, Ca^{2+}, Sc^{3+}, Ti^{4+}, V^{5+}, Cr^{6+}, Mn^{7+}. As the radius decreases and the charge increases, the electron-withdrawing tendency and the electronegativity of a cation increases, and thus it becomes increasingly difficult for protons to remain on the coordinated waters. The field of K^+ barely suffices to orient the surrounding water dipoles, whereas Ca^{2+} and Sc^{3+} hold eight and six waters, respectively, strongly enough to bring them into the lattice of some salts. The remaining ions remove protons from one, two, or four water molecules (cf. Table 6) of hypothetical hydrated ions, and form σ and π bonds with the protonless oxygens as described on p. 21. That this phenomenon is not merely a matter of ionic size and charge may be seen by comparing Ti^{4+} with Sn^{4+} and Al^{3+}. While the ionic radius of Sn^{4+} is very similar to (and that of Al^{3+} appreciably smaller than) that of Ti^{4+}, Sn^{4+} and Al^{3+} are coordinated, with O_h symmetry, to six water molecules, whereas Ti^{4+} is coordinated, with C_{4v} symmetry, to one oxygen and five water molecules. Unlike Ti^{4+}, Sn^{4+} and Al^{3+} do not have d orbitals available for the formation of π bonds with oxygen. In Sn^{4+} (Kr $4d^{10}$ configuration) the 5s and 5p orbitals are used for σ bonding, while the 5d ones lie too high in energy and are too diffuse to allow the formation of strong π bonds. Similarly, for Al^{3+} 3s and 3p orbitals are used for σ bonding, while 3d lies too high in energy. Pauling's electronegativity principle would suggest, however, that the water molecules are more firmly bound to Sn^{4+} and Al^{3+} than to the oxo- and dioxo-cations of Table 6, since the latter have their effective atomic charges reduced by σ and π bonding with protonless oxygens. It is evident from these considerations that only those ions that are large enough to accommodate six O^{2-} ions and that in acid solution coordinate to one or more proton-deficient oxygens (i.e., OH^- or O^{2-}) have the potential of forming ferro- and/or antiferroelectric perovskite-type oxides. A condition for the last requirement is that the ions must have low-lying and completely empty 3d ≲ 4s, 4p;

4d $\lesssim$ 5s, 5p; or 5d $\lesssim$ 6s, 6p acceptor orbitals available for combination with filled donor ones of O^{2-}. For example, $BaTiO_3$ becomes ferroelectric while $BaSnO_3$ does not, since not only a critical ionic size is involved but also orbitals for π-bond formation are needed.

Role of the Cuboctahedral-Coordinated Cation

The number of water molecules that may be accommodated around a cation is determined by its radius ratio, as given in Table 6 for La^{3+} and for alkali and alkaline earth ions found in perovskite-type oxides. Within this group only Ca^{2+}, Sr^{2+}, and La^{3+} have sufficiently large ratios of charge/radius to bring their full numbers of H_2O into the lattice of some salts. None of the remaining ions is able to orient all of its surrounding water dipoles. For example, as the size of the ion increases, $Ca^{2+} < Sr^{2+} < Ba^{2+}$, the charge remaining constant, the ability to polarize lone-pair orbitals of H_2O and thereby to attach these molecules by polar bonds decreases.[25]

Sr^{2+} in $SrTiO_3$ is surrounded by three more oxygens than in solution, while Ba^{2+} in $BaTiO_3$ is surrounded by the same number as in solution. In cuboctahedral O_h symmetry, the Sr^{2+} 5s, 5p, and 5d orbitals therefore overlap much less with the pair of 2p orbitals (σ and π about the Sr-O and Ti-O bond axes, respectively) on each ligand than do the Ba^{2+} 6s, 6p, and 6d ones with theirs (cf. Figs. 2, 3, and Table 1). Six σ bonds are involved in the cuboctahedral arrangement. Furthermore, Sr^{2+} holds these orbitals better than Ba^{2+} and thus prevents their involvement with Ti^{4+}. The decrease in cell volume of $SrTiO_3$ with lowering temperature does not lead to a piling-up of charge on Sr^{2+} from an increasing overlap which is so great that a transition to a ferroelectric state occurs.

In $CaTiO_3$ the distortion from the ideal structure is such that the octahedra pivot about their centers in order to bring six of their O^{2-} ions into closer contact with the Ca^{2+} ion; each Ti^{4+} ion is at the center of an octahedron which is centrosymmetric but not perfectly regular; each octahedron has the same shape, but neighboring octahedra are tilted with respect to one another.[26] Since the 3s, 3p, and 3d orbitals of Ca^{2+} polarize the pair of 2p orbitals (actually $p^{1-n}s^n$ hybrids because of the slight departure from 180° of the Ti-O-Ti bonds) on each O^{2-}, any π-bond formation between Ti^{4+} and O^{2-} is prevented.

No ferroelectric phase occurs in $BaZrO_3$ and $BaHfO_3$ because the larger Zr^{4+} and Hf^{4+} ions increase the O-O and Ba-O distances of the cuboctahedron, thereby

---

25) For an excellent discussion of hydrates see A. F. Wells, "Structural Inorganic Chemistry," 3rd ed., Oxford University Press, London, 1962, pp. 572 ff.

26) H. D. Megaw, Ref. 14, pp. 89 ff; H. F. Kay and P. C. Bailey, Acta Cryst. 10, 219 (1957).

reducing overlap. Like $SrTiO_3$, $SrZrO_3$ and $SrHfO_3$ are cubic,[27] or like $CaTiO_3$, orthorhombic.[28] $CaZrO_3$ and $CaHfO_3$ are probably isomorphous with $CaTiO_3$.[27] Because of the reasons given for their Ti^{4+} analogs, ferroelectric phases do not occur for these oxides. It is likely that $RaZrO_3$ and $RaHfO_3$ have ferroelectric phases but these compounds have not been studied because of their radioactivity.

Potassium niobate(V) ($KNbO_3$) shows the closest resemblance to $BaTiO_3$, having the same three ferroelectric forms with the transitions; cubic $\xrightarrow{410^\circ C}$ tetragonal $\xrightarrow{210^\circ C}$ orthorhombic $\xrightarrow{-40^\circ C}$ rhombohedral, while $NaNbO_3$ shows quite different dielectric behavior, with a number of forms of which at least one is antiferroelectric.[27] The lower polarizing power of Na^+ compared with Ca^{2+} allows the 2p orbital pair on some of the O^{2-} ions to become involved in π bonding with Nb^{5+}. In addition, the higher charge of Nb^{5+} requires greater charge neutralization from the ligand orbitals. A further analysis of this structure will be given in a future paper. That $KTaO_3$ and $NaTaO_3$[29] do not show the same behavior as $KNbO_3$ and $NaNbO_3$, respectively, is indeed puzzling because of the chemical similarity of Nb^{5+} and Ta^{5+}. A low-temperature investigation of $KTaO_3$ should be made; similarly, one of $RbTaO_3$ with a cubic $\xrightarrow{245^\circ C}$ tetragonal, (ferroelectric) transition for additional ferroelectric phases.

Analyses of perovskite-type oxides containing Pb^{2+} and Bi^{3+} in the cuboctahedral position will be given in a future paper. Dunitz and Orgel [30] have shown that such ions, with an outer, doubly occupied s orbital, differ from all other filled-shell ones in that they have a low-lying excited configuration (6s)(6p). If the s-p separation is sufficiently small, the regular environment is unstable. Although of smaller size than Ba^{2+}, these unsymmetrical ions, with a lone electron pair in an sp hybrid orbital, enhance off-center distortions in perovskite-type oxides.

Antiferroelectricity in WO_3

By removal of the cuboctahedral-coordinated cations from the perovskite-type structure, a ReO_3-type structure is obtained. Of the trioxides of the group VIA elements, WO_3 alone (although in distorted variants) adopts this simple structure in which only the corners of the octahedra are shared. Tungsten(VI) oxide is monoclinic[31] at ordinary temperatures and tetragonal[32] above 710°C.

---

27) H. D. Megaw, Ref. 14, pp. 89-103.

28) R. S. Roth, J. Research Natl. Bur. Standards 58, 75 (1957).

29) H. F. Kay and J. L. Miles, Acta Cryst. 10, 213 (1957).

30) J. D. Dunitz and L. E. Orgel, Ref. 2, pp. 40-44.

31) G. Andersson, Acta Chem. Scand. 7, 154 (1953); A. Magnéli et al., Final Tech. Rep. No. 1, Univ. of Stockholm, Inst. of Inorg. and Phys. Chemistry, Dec. 1960.

32) W. L. Kehl, R. G. Hay, and D. Wahl, J. Appl. Phys. 23, 212 (1952).

Other polymorphs have been found in the temperature range 200° to 300°C[33] and below -50°C.[34]

In tetragonal WO_3, each W^{6+} ion is displaced along a fourfold axis toward one corner of the octahedron, same as the Ti^{4+} ions in tetragonal $BaTiO_3$. The molecular-orbital description for the WO_6 group of C_{4v} symmetry is shown in Table 3 and Figs. 6 and 7, except that in the case of W^{6+} the 5d, 6s, and 6p orbitals are used for bonding. The W^{6+} displacements along each C_4 axis are interdependent and go in the same direction, for the same reason as the Ti^{4+} displacements in $BaTiO_3$. The C_4 chains in WO_3, unlike those in $BaTiO_3$, are in an antiparallel arrangement (i. e., each of the four neighboring chains has its W^{6+} displacements opposite to those of the central one), leading to antiferroelectricity. Since the square-planar O^{2-} ions are colinearly attached in WO_3 (but not in tetragonal $BaTiO_3$), the 2s orbital and one 2p orbital of each are hybridized to provide two equivalent $s^{1/2}p^{1/2}$ ones directed at 180°; these form ligand-σ molecular orbitals involved in bonding to the W^{6+} ions. The two remaining 2p orbitals of each square-planar O^{2-} ion are unchanged by the hybridization. One of these orbitals overlaps partly π and partly σ with $5d_{xz}$ (or $5\,d_{yz}$) orbitals on each of the colinearly attached W^{6+} ions, while the other overlaps entirely π with $5d_{xy}$ orbitals on each (Fig. 13). Since the negative lobe of the former 2p orbital overlaps largely with a $5d_{xz}$ (or $5d_{yz}$) negative lobe of one W^{6+} and the positive lobe largely with a $5d_{xz}$ (or $5d_{yz}$) positive lobe of the other W^{6+}, antiferroelectric coupling of the two W^{6+} ions is produced. The positive and negative lobes of the other 2p orbital overlap equally with $5d_{xy}$ positive and negative lobes, respectively, on each of the two W^{6+} ions. The participating orbitals of the partly σ, partly π combination are coplanar but not matched in sign everywhere in space, while those of the entirely π combination are not coplanar but matched in sign everywhere. This gives a W-O (square-planar)-W triple bond, much weaker than the W-O triple bond along the C_4 axis.

In acidic aqueous solution W^{6+} is present as the molecular species $[WO_2(H_2O)_4]^{2+}$ of D_{4h} symmetry (cf. Table 6). Since both protonless oxygens are strongly triple-bonded to W^{6+}, the remaining orbital directed outwardly from each is largely of s character. A D_{4h} arrangment cannot occur in WO_3 because each O^{2-} ion is attached to two W^{6+} ions. Rather the charge neutralization of W^{6+} is accomplished by one strong triple bond along the C_4 axis, four weak triple bonds with the square-planar oxygens, and one very weak predominantly ionic σ bond along the C_4 axis. (Compare with the bonding in tetragonal $BaTiO_3$, where Ti^{4+} for charge neutralization requires only σ bonding with the square-planar oxygens leading to ferroelectricity (pp. 11-12).

The W^{6+} displacements along C_2 axes in adjacent xz planes of the monoclinic

---

33) C. Rosen, E. Banks, and B. Post, Acta Cryst. 9, 475 (1956).

34) B. T. Matthias and E. A. Wood, Phys. Rev. 84, 1255 (1951).

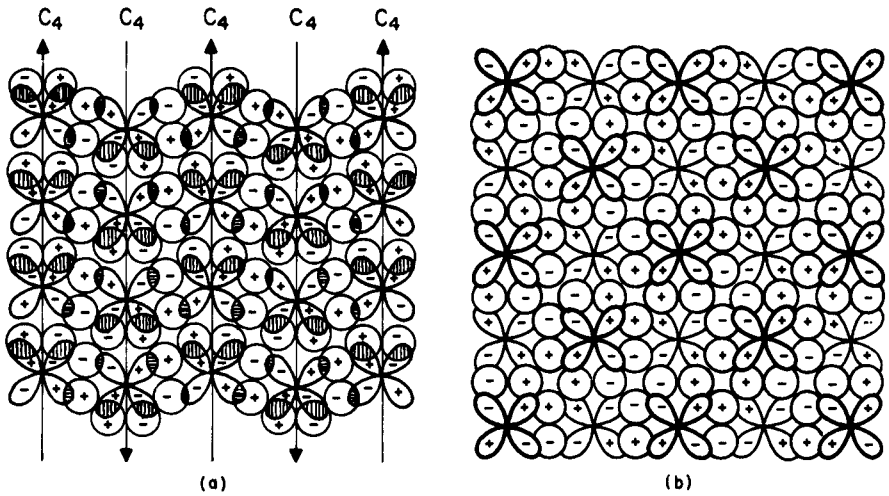

Fig. 13. Antiferroelectric coupling in tetragonal WO_3. (a) Overlap of W^{6+} $5d_{xz}$ (or $5d_{yz}$) with O^{2-} 2p; (b) overlap of W^{6+} $5d_{xy}$ with O^{2-} 2p.

modification of WO_3 alternate up and down (antiferroelectric coupling).[31] Each of the two 2p orbitals that remain after the sp hybridization of each yz-plane O^{2-} ion couples the $5d_{yz}$ and $5d_{xy}$ orbitals, respectively, of two colinearly attached W^{6+} ions, in the same manner as above. The transition to this phase occurs for much the same reason as that in $BaTiO_3$, but here the greater charge of W^{6+} requires the overlap provided by the pair of 2p orbitals on each yz-plane oxygen.

The structure of the ferroelectric modification of WO_3 reported by Matthias and Wood[34] to appear below -50°C is not known.

Conductivity and Overlap of t_{2g} d Orbitals

Ions containing d electrons in the valence shell (e. g., Ti^{3+}, V^{4+}, Cr^{3+}, Mn^{3+}, Fe^{3+}, Nb^{4+}, Mo^{5+}, Ta^{4+}, W^{5+}, Re^{6+}) do not form ferro- and/or antiferroelectric perovskites. Such electrons, lying in antibonding t_{2g}^* molecular orbitals, cancel the effect of π bonds (needed for ferro- and antiferroelectricity), since an antibonding orbital is more relaxing than a bonding one is binding. In compounds such as $Ba_{1-x}^{2+}La_x^{3+}Ti_{1-x}^{4+}Ti_x^{3+}O_3$, $K_{1-x}^{+}Ba_x^{2+}Nb_{1-x}^{5+}Nb_x^{4+}O_3$, and $Na_x^{+}W_{1-x}^{6+}W_x^{5+}O_3$ off-center distortions disappear, the cubic modification results, and the cell volume increases when a sufficient number ($0 < x < 1$) of electrons is added to the antibonding orbitals. Metallic-type conductivity occurs because the O^{2-} πp orbitals no longer or very weakly involved in bonding with the octahedral-coordinated cations allow the t_{2g} or t_{2g}^* orbitals of neighboring cations to overlap exclusively with one another and thereby provide a narrow conduction band into which x electrons are introduced (Fig. 14).

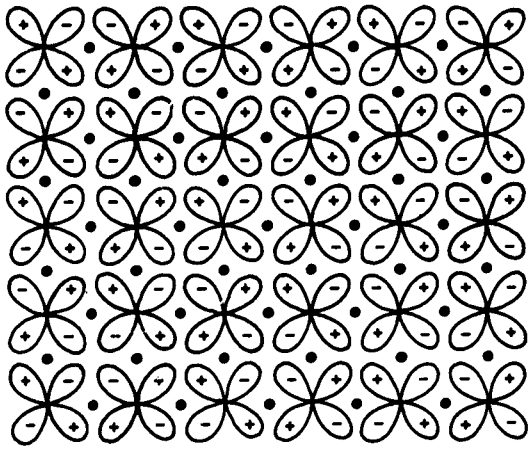

Fig. 14.

Overlap of neighboring cation t_{2g}^* (π antibonding combination of cation t_{2g} and O^{2-} $2p\pi$) or t_{2g} (nonbonding cation t_{2g} and O^{2-} $2p$) d orbitals to provide a conduction band.

The d orbitals become more contracted as the nuclear charge (atomic number) increases by moving across a transition-metal series (e.g., Ti, V, Cr, Mn, Fe, Co, Ni). On the other hand, they become more extended as the ionic charge (oxidation-state number) of a transition metal increases (e.g., Ti^{o}, Ti^{2+}, Ti^{3+}, Ti^{4+}), because the greater the polarization of electrons in anion orbitals toward the cation, the larger the cation-anion orbital overlap, and the more effective the screening of d electrons from each other and from the cation nucleus. They become more extended, too, as the principal quantum number increases (e.g., Ti^{4+}, Zr^{4+}, Hf^{4+}), because of an increasing number of radial nodes: zero for 3d, one for 4d, and two for 5d. Illustrations of these trends are afforded by absorption-spectra studies.[35, 36]

For a number of compounds Morin[36] has calculated overlap integrals of t_{2g} orbitals on neighboring cations where the effective charge of a cation, as determined by Slater's rules, is corrected for additional screening due to overlap. The only perovskite-type oxides included in his results are $Ba_{0.5}TaO_3$, WO_3, and $Na_{0.7}WO_3$, for which the overlap integrals give a conduction band; the first two are insulators in that the band is normally empty. These results and the location of Ti, Zr, Hf, Nb, Ta, Mo, and W in the periodic table suggest that their perovskites have a conduction band into which electrons are placed by substitution in either the cuboctahedral or octahedral positions with cations of higher oxidation state for those which are present in their highest oxidation state (e.g.,

---

35) D. S. McClure, Ref. 8, pp. 449-451, 507-511.

36) F. J. Morin, J. Appl. Phys., Suppl., 32, 2195 (1961); Phys. Rev. Letters 3, 34 (1959); Bell System Tech. J. 37, 1047 (1958).

$Ba^{2+}_{1-x}La^{3+}_{x}Ti^{4+}_{1-x}Ti^{3+}_{x}O_3$, $La^{3+}_{0.67+x}Ti^{4+}_{1-3x}Ti^{3+}_{x}O_3$, $Ba^{2+}_{0.5+x}Ta^{5+}_{1-2x}Ta^{4+}_{2x}O_3$, $Ba^{2+}Ti^{4+}_{1-2x}$-

$Ti^{3+}_{x}Nb^{5+}_{x}O_3$, $K^{+}Ta^{5+}_{1-2x}Ta^{4+}_{x}W^{6+}_{x}O_3$, $Na^{+}_{x}W^{6+}_{1-x}W^{5+}_{x}O_3$). The stoichiometric cubic perovskites $SrMoO_3$ and $BaMoO_3$ are metal-like conductors with positive-temperature coefficients of resistivity;[37] each Mo^{4+} supplies two electrons to the conduction band. Conduction in ReO_3, where each Re^{6+} would contribute one electron to the band, is probably of the metallic type. Electron mobility in ReO_3 is expected to be lower than that in Na_xWO_3 because an increase in nuclear charge (atomic number) brings about less overlap of neighboring cation t_{2g} orbitals.

The d electrons of the ions such as Cr^{3+}, Mn^{3+}, Fe^{3+}, and Co^{3+} do not provide conductivity in perovskite-type oxides since the effect of nuclear charge predominates, making their d orbitals so localized that sufficient overlap cannot occur. These oxides have interesting magnetic properties.[38] If solid-state solutions of a perovskite which is ferro- or antiferroelectric with one which has an ion following V in the 3d row or an ion of a group VIII element (all of which when in an octahedral-oxide surrounding contain d electrons in the valence shell) are prepared, conductivity does not increase but the ferro- or antiferroelectric effect is diluted with increasing concentration of the latter perovskite.

Conclusions

The theory of ferroelectricity and antiferroelectricity in perovskite-type oxides advanced here differs from others in its emphasis on short-range forces and its neglect of long-range ones. (Similarly, from a molecular point of view, Slater[39] successfully treated ferroelectricity in KH_2PO_4 by recognizing the vital role played by the hydrogen bonds.) The phenomenon is also encountered in many complex oxides not of the perovskite type. The theory in its present form is applicable to those structures having octahedra linked by their corners only and having large holes which accommodate atoms less strongly bonded to the framework. Examples of complex oxides having such structures are dicadmium diniobate(V) ($Cd_2Nb_2O_7$) of the pyrochlore type and lead(II) diniobate(V) ($PbNb_2O_6$) of the tetragonal tungsten-bronze type. The occurrence of ferroelectricity in a series of mixed bismuth oxides with the general formula $[Bi_2O_2]^{2+}[Me^{a}_{m-1}Me^{b}_{m}O_{3m+1}]^{2-}$ (where Me^{a} = ions of appropriate size and oxidation state; Me^{b} = Ti^{4+}, Nb^{5+}, Ta^{5+}, etc., either singly or in combination; and m = 2, 3, 4, etc.), based on sequences of

37) L. H. Brixner, J. Inorg. Nucl. Chem. 14, 225 (1960).

38) M. A. Gilleo, Acta Cryst. 10, 161 (1957); P. W. Anderson, "Theory of Magnetic Exchange Interaction: Exchange in Insulators and Semiconductors," in Solid State Physics, Vol. 14, F. Seitz and D. Turnbull, Eds., Academic Press, New York, 1963, pp. 99-214; J. B. Goodenough, "Magnetism and the Chemical Bond," Interscience Publishers, John Wiley and Sons, New York, 1963.

39) J. C. Slater, J. Chem. Phys. 9, 16 (1941).

$[Bi_2O_2]^{2+}$ layers interleaved with portions of perovskite-like structure,[40] may also be considered from a molecular point of view. Note that the arrangement of atoms within the $[Bi_2O_2]^{2+}$ layers is the same as that in tetragonal PbO, and that Pb^{2+} and Bi^{3+} have identical electronic configurations.

Since the atomic positions in the structure of these oxides must be known for the kind of analysis presented here, additional X-ray and neutron-diffraction work is necessary. Spectral studies of oxo- and dioxo-cations (cf. Table 6, p. 23) in oxalato compounds and in strong acid solution, and similarly of oriented thin films of $BaTiO_3$ and other oxides should be very instructive. Overlap integrals may be evaluated for the structures in which the atomic positions are known and estimates of the degree of covalency present may be determined by the methods outlined by Ballhausen.[41]

More nuclear-magnetic and nuclear-quadrupole resonance experiments on these materials should be done. Results from such experiments by Cotts and Knight[42] on $KNbO_3$ indicate that the direction and magnitude of the field gradient at Nb^{5+} cannot be predicted from an ionic model based on point charges; it appears that covalent bonding, where the field gradient is generated by valence electrons that penetrate the ion core, has to be assumed. The present paper might be helpful in the further understanding of their results. In addition, their experiments show that in the cubic phase the equilibrium position of Nb^{5+} is at the center of the oxide octahedron; this is inconsistent with the view that there are permanent dipoles in the lattice and thus six equilibrium positions for Nb^{5+}, but in full agreement with the model presented here.

Experiments have been proposed by Newnham[43] to explore in ferroelectric transitions the role of ions that exhibit a Mössbauer effect.

Acknowledgment

The author wishes to express his appreciation to Professor A. von Hippel for constant encouragement and to Professor W. N. Lipscomb of Harvard University for having provided notes on group theory in its applications to chemical problems. Thanks are due to Professor R. E. Newnham for valuable discussions.

Many of the ideas in this report were independently originated by Professor Lipscomb.

---

40) B. Aurivillius, Arkiv Kemi 1, 463 and 499 (1949); 2, 519 (1950); E. C. Subbarao, J. Am. Ceram. Soc. 45, 166 (1962).

41) C. J. Ballhausen, Ref. 10, pp. 159-177.

42) R. M. Cotts and W. D. Knight, Phys. Rev. 96, 1285 (1954).

43) R. E. Newnham, private communication.